Mater.Phys.Mech.1 (2000) 31-38

ENHANCED DIFFUSION NEAR AMORPHOUS GRAIN BOUNDARIES IN NANOCRYSTALLINE AND POLYCRYSTALLINE SOLIDS

R.A. Masumura[1] and I.A. Ovid'ko[2]

[1]Naval Research Laboratory, Washington, DC 20375, USA
[2]Institute of Problems of Mechanical Engineering,
Russian Academy of Sciences, Bolshoi 61, Vas. Ostrov, St. Petersburg, 199178, Russia

Received: September 23, 1999

Abstract. A theoretical model is constructed that describes diffusion processes enhanced by the elastic interaction of the diffusing species and amorphous grain boundaries in nanocrystalline and polycrystalline solids. A partial differential equation governing evolution of the spatially inhomogeneous concentration of the diffusing species near amorphous grain boundaries is numerically solved. It is shown that the enhanced diffusion essentially influences the growth of amorphous grain boundaries in solids under irradiation and thermal treatment as well in sintered ceramics and is capable of contributing to the anomalously fast diffusion in nanocrystalline solids.

1. INTRODUCTION

The process of the diffusion, where one species rearranges its configuration in a lattice (a solid in this case) in response to an external force, is an attempt to approach equilibrium. When a concentration gradient exists as the only driving force, this irreversible process can be concisely formulated leading to a second order parabolic partial differential equation (PDE). The solution of this PDE has been determined for many types of boundary and initial conditions and geometries.

If additional driving forces are present due to electrical, magnetic, thermal or elastic fields, the appropriate PDE can be formulated subject to simplifying assumptions. The question now becomes, whether this additional driving force will enhance or retard the flow of diffusing species thorough the lattice. In particular, we are interested in the effect of an amorphous intergranular boundary dislocation stress field has on the diffusion of various species in nanocrystalline and polycrystalline solids. Such boundaries frequently exist in sintered nanostructured and polycrystalline ceramics [1-5] as well in monophase and composite solids under irradiation and thermal treatment, where diffusion- and irradiation-induced amorphization processes often start to occur at grain boundaries [6,7]. Amorphous grain boundaries in sintered ceramics are characterized by a chemical composition that is different from that of adjacent crystalline grains as well by a nano-scaled thickness whose value is essentially constant within a ceramic sample. These grain boundaries are dependent on only the chemical composition and insensitive to misorientation parameters of the boundaries (see [1,8] and references therein). Amorphous grain boundaries in monophase and composite solids under irradiation and thermal treatment play the role as nuclei for enhanced diffusion- and irradiation-induced amorphization, where the boundaries transform into extended amorphous layers with the meso- and macroscale thickness growing parallel with the diffusion and irradiation processes [6,7]. Recently, a model [9,10] has been suggested describing the role of elastic distortions in the formation of amorphous grain boundaries. This model, however, does not quantitatively take into account the effect of diffusion on evolution of amorphous grain boundaries after they have been formed. At the same time, this effect is important for an adequate description of both the structural features and the properties of nanocrystalline and polycrystalline solids containing amorphous grain boundaries.

The model presented here is an initial attempt to understand the role of enhanced diffusion in evolution of amorphous grain boundaries in (i) sintered ceramics and (ii) monophase and composite solids under irradiation and thermal treatment. The model also is concerned with the contribution of amorphous grain boundaries to enhanced diffusion in nanostructured solids (often exhibiting the outstanding diffusional

Corresponding author: I.A. Ovid'ko, e-mail: ovidko@def.ipme.ru

properties [11,12]), which is related to elastic interaction of amorphous grain boundaries and the diffusing species. As such, we have assumed that the crystalline grains are separated by an amorphous grain boundary layer that provides the source of the diffusing species. To retain the flavor of dislocation model of a simple tilt boundary, we will consider that a double wall of dislocations separate the amorphous layer. We further assume that dislocations do not interact with each other.

We will discuss the development of the appropriate PDE and the elastic interaction from a double wall of dislocations. This will lead to the formulation of the interaction energy that will be used in the PDE whose solution is determined numerically. Finally, we will discuss the results of the numerical analysis.

2. MATHEMATICAL FORMULATION

The flux or current density of a diffusing species in the presence of a concentration gradient is given as,

$$\vec{j} = -D\nabla C, \tag{1}$$

where D is the diffusivity and C is the concentration. If there is an elastic interaction between the diffusing species and a stress field in a homogenous, linear and isotropic solid, Eq. 1 is modified as [13]

$$\vec{j} = -\left[D\nabla C + \frac{C}{kT}\nabla\varepsilon \right], \tag{2}$$

where ε is the interaction energy, k is Boltzmann's constant and T is the absolute temperature of the diffusion process. It is assumed that the mobility μ, caused by the force from the strain gradient is the same as in the chemical potential force,

$$\mu = \frac{D}{kT}. \tag{3}$$

It will be assumed that the diffusivity is constant and independent of both concentration and strain.

Using the continuity equation, Eq. 2 can be recast as

$$\frac{\partial C}{\partial t} = D\left(\nabla^2 C + \frac{1}{kT}\nabla C \cdot \nabla\varepsilon \right), \tag{4}$$

since

$$\nabla^2\varepsilon = 0, \tag{5}$$

due to the absence of any internal body forces. Eq. 4 along with the appropriate initial and boundary conditions will be solved to determine how the concentration is affected by the elastic interaction.

A formulation for the interaction energy based upon a grain boundary model is required. For nanocrystalline and polycrystalline materials, an appropriate model is the one proposed by Kolesnikova et al. [9] and Ovid'ko and Reizis [10] where an amorphous grain boundary layer occurs as described below between the nanosized grains.

3. DOUBLE WALL MODEL

In the framework of dislocation-structural-unit models [14,15], a conventional tilt grain boundary in a crystal can be treated as a periodic wall array of edge grain boundary dislocations whose spatial positions and Burgers vectors are strictly determined by parameters (misorientation, etc.) of the boundary. In this model representation, the elastic fields and the elastic energy density of a tilt boundary are those of the corresponding array of grain boundary dislocations [16,17]. Following [9,10], transformation of a conventional tilt grain boundary into an amorphous grain boundary is associated with a re-arrangement of its grain boundary dislocation ensemble. In doing so, due to the fact that the amorphous disordered structures do not impose strict limitations on both spatial positions and Burgers vectors of grain boundary dislocations, such dislocations in a new, amorphous boundary are arranged in the way decreasing their elastic energy density. The discussed decrease of the elastic energy density causes the basic driving force F_{el} for the transformation of a conventional tilt boundary into an amorphous boundary. This force is calculated in the model [9,10] which to a first approximation describes the amorphous boundary to be of finite width, λ, with dislocation arrays at each of the interfaces between amorphous and the crystalline grain as shown in Fig. 1. Following the

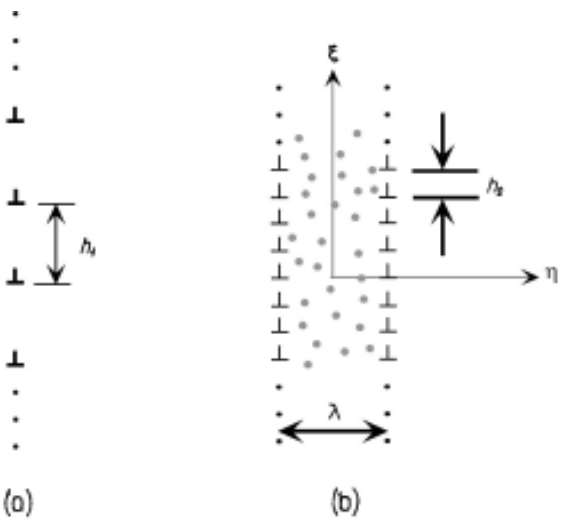

Fig. 1. (a) Single dislocation array and (b) double wall with amorphous grain boundary of width λ.

calculations of references [9] and [10], the driving force F_{el} is large at $\lambda \le h_2$ and $\cong 0$ at $\lambda > h_2$, where h_2 is the period of the dislocation walls (Fig. 1). The elastic interaction between the two dislocation walls exists in only the range of $\lambda \le h_2$; the walls, in general, do not interact elastically at $\lambda > h_2$. As a corollary, evolution of the amorphous grain boundary at $\lambda = h_2$ is caused by the thermodynamic force F' related to other factors other than the decrease of the elastic energy density. More precisely, the force F' is as follows [10]:

$$F' = -\varepsilon_{a-c}(\lambda) - (2\kappa + \lambda)\frac{d\varepsilon_{a-c}}{d\lambda}, \tag{6}$$

where ε_{a-c} denotes the difference between the free energy densities of the amorphous and crystalline phases, and k the characteristic spatial scale of structural inhomogenities in the amorphous phase. The term ε_{a-c} strongly depends on the chemical composition which, in general, is spatially inhomogeneous in the vicinity of the amorphous boundary and can evolve in time due to diffusion. In these circumstances, the F'-induced evolution of the amorphous grain boundary is sensitive to the diffusion processes in its vicinity. On the other hand, the stress field of the boundary influences the diffusion processes and, as a corollary, evolution of the boundary. The elastic interaction between the diffusing species and the stress field is related to the sum of the normal stresses. For a double wall of non-interacting dislocation infinite arrays a distance λ apart the sum of the normal stresses is,

$$\sigma_{ii} = -\frac{Gb_2(1+\nu)}{2(1+\nu)h_2}\omega(2\pi\xi), \tag{7}$$

where

$$\omega(\eta,\xi) = \frac{\sin(2\pi\xi)}{\cosh\{2\pi(\eta - \frac{\lambda^*}{2})\} - \cos(2\pi\xi)} + \frac{\sin(2\pi\xi)}{\cosh\{2\pi(\eta + \frac{\lambda^*}{2})\} - \cos(2\pi\xi)}, \tag{8}$$

and letting $\eta = x/h_2$, $\xi = y/h_2$ and $\lambda^* = \lambda/h_2$ for the coordinate system given in Fig. 1 where the dislocation walls are symmetrical located at $x = \pm\lambda/2$. The shear modulus and Poisson's ratio are denoted by G and ν, respectively.

4. INTERACTION ENERGY

We assume the volume of the diffusing and host species are different and thus giving rise to an elastic interaction. On the average, let ΔV be the volume change and this volume difference interacts with a homogenous applied stress field. It can be shown that the elastic interaction is given as

$$\varepsilon = (\Delta V)\Theta, \tag{9}$$

where $\Theta = -\sigma_{ii}/3$, the hydrostatic component of the stress field. This interaction will alter the total energy of the system depending upon the sign of the product.

In Fig. 2a is plotted the contours of constant normalized interaction energy (i.e., $\omega(\eta,\xi)$) for a strip $|\xi| \le 0.5$. As expected, a large energy gradient exists near the dislocation, $\xi=0$ due to the elastic singularity of the dislocation core. Depending upon the volume change, this elastic interaction will enhance diffusion. For illustrative purposes, it will be assumed that $\Delta V > 0$. In Fig. 2a, from a qualitative viewpoint, the diffusing species would to migrate below the extra dislocation half plane to lower their total energy. A spherical point defect interacting with a single edge dislocation also exhibits this behavior [18].

The force, $\bar{f}$, on the migrating specie is determined from $-\nabla\varepsilon$ and the results are shown in Fig. 2b for the corresponding interaction energy of Fig. 2a. The diffusing specie will tend to move away from above the dislocation and migrate to the edge of the extra half plane of the dislocation. This periodic case of a tilt boundary is different from that for an isolated edge dislocation in that the diffusing specie in the upper one fourth of the strip diffuses to the next strip above. This is only a qualitative assessment and should serve as guide when a concentration gradient is not considered.

5. NUMERICAL SOLUTION

Before solving Eq. 4, the initial and boundary conditions must be specified. We need to only consider one strip, $|\xi| < 1/2$, since we assume the grain boundary to be modeled by an infinite array of dislocations and can utilize a periodic boundary condition, $C(\eta,-1/2,t) = C(\eta,1/2,t)$ for $\eta \ge 0$. We will assume that the amorphous layer in between the nanosized grains will be an undiminished source of the diffusing specie, thus, $C(0,\xi,t) = 1.0$ for $|\xi| < 1/2$. Since the dislocation stresses from a regular array are short range in nature, it is reasonable to utilize $C(\infty,\xi,t)=0$ in each and every strip. The above boundary conditions are valid for $t > 0$. For an initial condition, we will assume that each strip is devoid of any of the diffusing specie at $t = 0$ leading to $C(\eta,\xi,0) = 0$.

Eq. 4 is normalized for computational purposes by rescaling time and letting the material coefficients become

$$\tau = Dt \text{ and } \gamma^* = \frac{DGb_2(1+\nu)}{2kt(1-\nu)h_2}. \tag{10}$$

The normalized computational form becomes

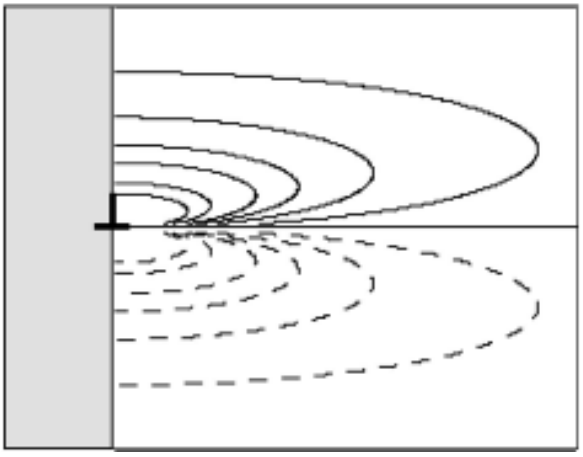

Fig. 2(a) shows the normalized interaction energy, ω. Above the dislocation, ω>0 (solid) while below ω<0 (dashed) for $\Delta V>0$. The area to the left of the dislocation is one half of the amorphous layer.

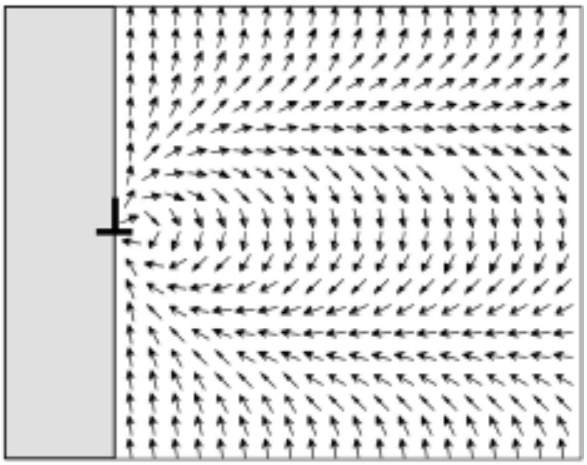

Fig. 2(b) indicates the flow of diffusant ($\Delta V>0$) corresponding to interaction energy shown in Fig. 2a as determined from $-\nabla\omega$. For clarity, each vector is normalized to one. The forces away from the dislocation are greatly attenuated. The area to the left of the dislocation is one half of the amorphous layer.

$$\frac{\partial C}{\partial \tau} = \nabla^2 C + \gamma^* \nabla C \cdot \nabla \omega \tag{11}$$

with the boundary conditions for $t > 0$,

$$C(\eta,-1/2,\tau) = C(\eta,1/2,\tau) \text{ for } \eta \geq 0, \tag{12}$$

$$C(0,\xi,\tau) = 1.0 \text{ for } |\xi| < 1/2, \tag{13}$$

$$C(\infty,\xi,\tau) = 0 \text{ for } |\xi| < 1/2, \tag{14}$$

and the initial condition at $\tau = 0$,

$$C(\eta,\xi,\tau) = 0 \text{ for } \eta > 0 \text{ and } |\xi| < 1/2. \tag{15}$$

An alternating-direction-implicit (ADI) method is utilized to obtain a numerical solution of Eq. 11. Each time step is divided equally in half. In the first half, a partial solution is determined by reducing the PDE to a one-dimensional problem in one of the orthogonal coordinates while keeping the other fixed. In the second half, the PDE is now solved in the other coordinate direction using the partial results obtained in the first half time step. This algorithm has the advantage of requiring a tridiagonal equation solver and is relatively stable (unconditionally if the coefficients of the PDE are constant). The η-direction partial solution requires a slight modification to the tridiagonal solver to account for periodic nature of the boundary conditions but it still retains the usual banded form. We have chosen to do the analysis first in the η-direction since the elastic fields are short-ranged in ξ.

The finite difference equations are based upon the usual five atom centered-computational molecule to approximate the Laplacian (spatial coordinates) and a two point approximation for the temporal first derivative. Using equal increments for the spatial coordinates, $\Delta\xi = \Delta\eta$ and utilizing a normalized time increment $\Delta\tau$, and rescaling γ for computation clarity,

$$\gamma^* = 4\gamma(\Delta\xi), \tag{16}$$

Eq. 12 can be approximated by finite difference form amenable for numerical computation.

For the actual computation, a strip $|\xi| \leq 1/2$ high and $0 \leq \eta \leq 3$ was used. The grid for this rectangle was divided into 100 and 300 equal increments for the ξ- and η-directions, respectively. The singularity of stress field was avoided by placing the dislocation in between the grid points. For each time step, the mass accumulation, $M(t)$, was determined by numerically integrating the normalized concentration over the computational rectangle.

To check the accuracy of the numerical scheme, an initial run was made with the interaction set to zero. This case corresponds to diffusion between two planes (one-dimensional problem). These results agreed with the analytical solution lending confidence to the numerical algorithm. Runs were made to explore the effect of the elastic interaction between grain boundary dislocations and diffusing species. First was to determine the role of the "strength" of the interaction as manifested through γ^* and second was to determine the effect of spacing between the dislocations (width of amorphous layer) in the wall, λ, on the diffusion process.

A typical run for values of $\gamma^* = 3$ and $\lambda = 1$ is shown in Fig. 3 for various normalized times. The concentration is larger above the dislocation since the flow lines from Fig. 2a indicate diffusion away from this area

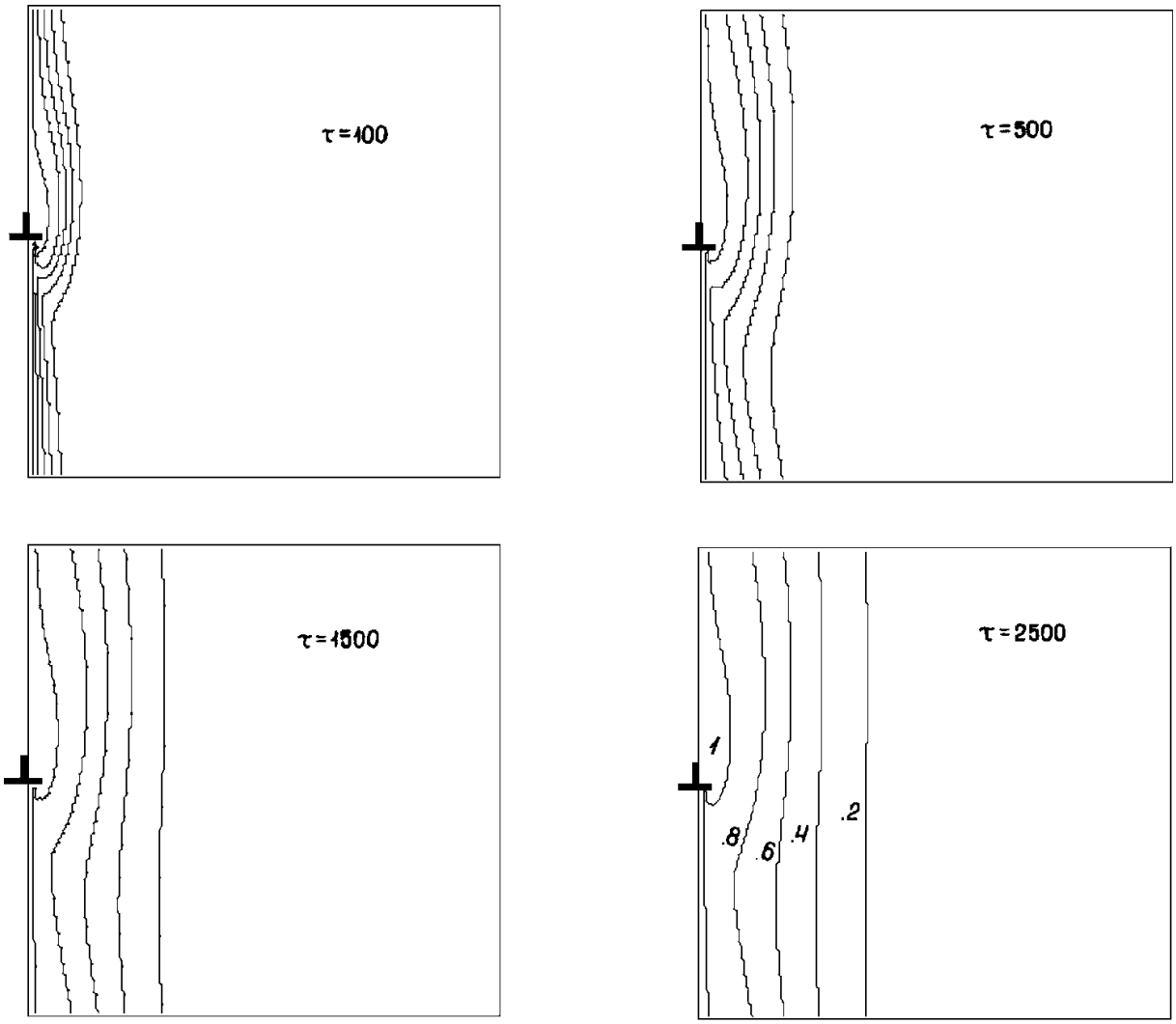

Fig. 3. Normalized concentration contours for various normalized times with and without elastic interaction. The values of $\gamma^* = 3$, $\lambda = 1$ and $\gamma^* = 0$, $\lambda = 1$ were used. The normalized contours have the same range of values for each time slice. The amorphous layer and other dislocation wall are not shown. The zero interaction case is the smaller segment with the uniform contours.

while the concentration is greatly diminished below the dislocation. The flow pattern generated from the static case, Fig. 2b indicates flow away from the interface above the dislocation and flow to the interface below the dislocation due to the elastic interaction. The concentration gradient would prefer to have a uniform flow (no x variation) but cannot overcome the elastic interaction particularly near the singularity at the dislocation. The diffusing specie accumulates below the extra half plane (recall, $\Delta V > 0$) and diffuses very rapidly to this area due to the mathematical singularity. Some the diffusant originates from the strip below as can be seen from the Fig. 2b. However the diffusing specie attempts decreases its concentration in the region above the extra half plane but cannot do so due to its source at the amorphous-crystalline interface. Thus, it flows over a larger area at nearly the maximum concentration in response to the elastic interaction enhancing the diffusion process. A fraction of the diffusant also flows to the strip above this one.

At later times, the diffusing specie is not effected by the elastic interaction due to the short-ranged effect of the grain boundary dislocation elastic fields. Away from the dislocation, the concentration profile becomes flat indicating a decreased influence of the elastic fields. Note however, at even these later times, the elastic interaction near the dislocation remains large as can be seen in Fig. 3. (In Fig. 3, the iso-contour lines have the same range of values for the various time slices.) For comparison, the zero interaction case, $\gamma^* = 0$, is shown in Fig. 3 in the small segment. As expected, the iso-contours are planar for this one-dimensional case. As can been seen from this figure, the iso-contours lines when $\gamma^* = 0$ lag behind the interaction cases and hence affect the mass accumulation of the diffusant.

The presence of the stress field from a grain boundary dislocation affects the mass accumulation. In Fig. 4

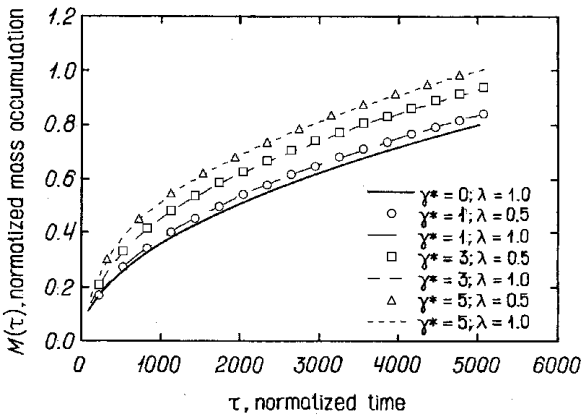

Fig. 4. Normalized mass accumulation for several values of γ^* and λ.

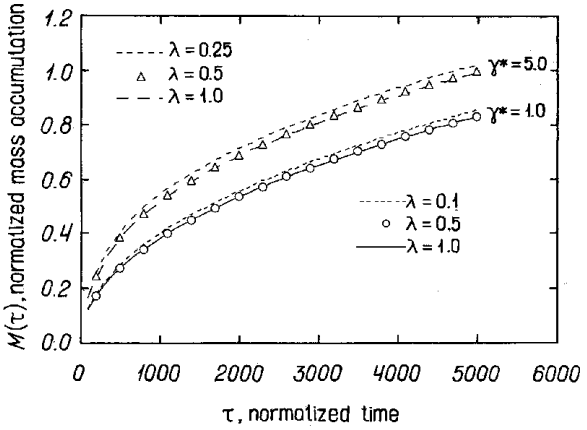

Fig. 5. Effect of width of dislocation wall spacing on mass accumulation.

is plotted the mass accumulation for several combinations of $\gamma^* = 0$, 1, 3 and 5 and $\lambda = 0.5$ and 1. There are several salient features to note. First, as expected, the amount of mass diffusion is increases with increasing elastic interaction, i.e., larger γ^*. Second there is very little discernable difference between $\lambda = 0.5$ and $\lambda = 1$ indicating that the short-range field effects are limited at these widths. Third, there is an enhanced diffusion over the base line case of $\gamma^* = 0$ of the order of 20% at the later times. Given the little effect of l on the mass diffusion, the baseline results for $\gamma^* = 0.5$ or 1 should be about the same. For that reason, we have shown only $\lambda = 1$ for $\gamma^* = 0$.

The width effect, e.g., the spacing between the dislocation walls has a marginal effect as the spacing, λ, becomes smaller. In Fig. 5, λ is varied from 0.1, 0.5 and 1 for two values of $\gamma = 1$ and 5. There is a slight increase in mass accumulation as the width is decreased to a value of 0.1 (recall this means that the spacing of the dislocation in each wall or array is 10 time larger that the separation distance between the walls). This analysis should be treated only as an indication of effect of the elastic interaction because this analysis uses the assumption of non-interacting dislocations.

4. DISCUSSION

We discuss the evolution of amorphous grain boundaries in (i) sintered ceramics and (ii) solids under irradiation and thermal treatment based on the role of enhanced diffusion. To do so, we assume that the species diffusing from a pre-existent amorphous grain boundary into adjacent crystalline regions are capable of inducing the amorphization of these regions. This corresponds to experimentally observed situations (i) [1-5] and (ii) [6,7] where diffusion mixing causes growth of the amorphous phase at grain boundaries. With the above taken into account, the following scenario of the evolution is suggested which takes into consideration the role of enhanced diffusion in amorphizing transformations at grain boundaries. Penetration of the "amorphizing" diffusing species from an amorphous grain boundary to adjacent crystalline regions occurs in a spatially inhomogeneous way (see previous sections and Fig. 6a) and leads to change of $\varepsilon_{a\text{-}c}$ in the regions with a high density of the amorphizing diffusing species. This induces amorphization (crystal-to-glass transition) in these regions (Fig. 6b). The spatially inhomogeneous growth of the amorphous phase (Fig. 6b) forces crystalline-amorphous interface to be curved and, therefore, results in an increase of its contribution to the total energy density of the amorphous boundary. The crystalline-amorphous interface can straighten out and, as a corollary, decrease the total energy density in the following two-step way. First, grain boundary dislocations, due to absence of structure-imposed limitations on their spatial positions, move to new positions (Fig. 6c). The dislocations located in new positions create a new stress

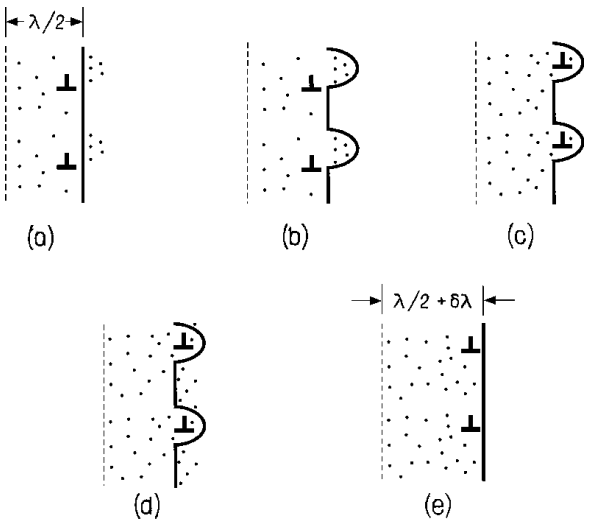

Fig. 6. Increased width of layer, $\delta\lambda$, by amorphization due to enhanced diffusion.

field distribution which, in its turn, enhances penetration of the amorphizing diffusing species from the amorphous grain boundary to new crystalline regions located between the "bugles" of the boundary (Fig. 6d). The diffusion is followed by amorphization of these new regions, in which case the crystal/glass interface becomes planar (Fig. 6e).

If there is a permanent "supply" of the amorphizing diffusing species to the amorphous grain boundary due to grain boundary diffusion (which quickly transfers the amorphizing diffusing species from some remote permanent source, e.g. a second phase region consisting of chemical elements that serve as the amorphizing diffusing species) or irradiation (see situation (ii)), then the boundary plays the role as a permanent source of the amorphizing diffusing species that penetrate into the adjacent crystalline grains. In these circumstances, the process shown in Fig. 6 is permanently repeated resulting in diffusion- or irradiation-induced permanent growth of the amorphous grain boundary. This corresponds to experimentally observed [6,7] situation (ii) where the diffusion- and irradiation-induced growth of the amorphous phase starts occurring at grain boundaries, which then gradually extend to amorphous regions of macro-scale extent.

If the quantity of the amorphizing diffusing species is limited, as in situation (i) with sintered ceramics, the process shown in Fig. 6 results in formation of an amorphous boundary of finite width. The boundary width is determined only by the sum (finite) quantity of the amorphizing diffusing in a sample. Since grain boundary diffusion is faster by several orders than bulk diffusion (that controls the growth of amorphous grain boundaries; see Fig. 6), basically, the same quantities of the amorphizing diffusing species are distributed along all the grain boundaries within a sample. This explains the experimentally observed (see [1,8] and references therein) specific feature of amorphous grain boundaries in sintered ceramics, which is a finite boundary width whose value is tentatively the same for all amorphous grain boundaries within a ceramic sample and depends on only the chemical composition.

The diffusion processes enhanced due to the elastic interaction of the diffusing species and amorphous grain boundaries represent an example of diffusion processes dependent on stress field distributions in polycrystalline and nanocrystalline solids. The contribution of such processes to the macroscopic diffusional properties is significant in solids with evolving defect structures and, therefore, evolving stress field distributions. In particular, the enhanced diffusion which accompanies transformations of amorphous grain boundaries (Fig. 6) is capable of essentially contributing to the anomalously fast diffusion in nanocrystalline solids where evolving (amorphous and conventional) grain boundaries are inherent structural elements.

4. CONCLUSIONS

As an initial to attempt to under the role of grain boundaries and their effect in nanosized materials, we have modeled a simple case of two non-interacting grain boundary arrays or walls separating an amorphous layer that provides a source for the diffusing species. A simple elastic interaction is considered and inserted into the diffusion equation that is solved for the time dependent behavior of the concentration. The mass accumulation is enhanced due to the elastic interaction and that until the spacing becomes small, the second dislocation array or wall has a minimal effect. And lastly, the static information derived from the interaction energy and its gradient, e.g. force on the diffusing specie, will only yield qualitative information and that time dependent analysis is required. The enhanced diffusion essentially influences the growth of amorphous grain boundaries in solids under irradiation and thermal treatment as well in sintered ceramics and is capable of contributing to the anomalously fast diffusion in nanocrystalline materials.

ACKNOWLEDGEMENTS

We wish to thank the Office of Naval Research Headquaters (ONR) and Office of Naval Research International Research Field – Europe (ONR-Europe) for their generous support. One of us, (I.A.O.) was the recepient of ONR grant N00014-99-1-0569) and of ONR-Europe grant N00014-99-1-4016. The other author, (R.A.M.), was supported by ONR grant N0001499AF00002.

REFERENCES

[1] Y.Kinemuchi, T.Yanai and K.Ishizaki // *Nanostr. Mater*. **9** (1997) 23.
[2] X.Pan // *J. Am. Ceram. Soc.* **79** (1997) 2975.
[3] H.Gu, X.Pan, I.Tanaka, R.M.Cannon, M.J.Hoffmann, H. Mullejans and M.Ruhle // *Mater. Sci. Forum* **207-209** (1996) 729.
[4] X.Pan, M.Ruhle and K.Nihara // *Mater. Sci. Forum* **207-209** (1996) 761.
[5] H.-J.Kleebe, G.Pezzotti and T.Nishida // *J. Mater. Sci. Lett.* **16** (1997) 453.
[6] M.A.Hollanders, B.J.Thijsse and E.J.Mittenmejer // *Phys. Rev. B* **42** (1990) 5481.
[7] W.L.Gong, L.M.Wang and R.C.Ewing // *J. Appl. Phys*. **81** (1997) 2570.
[8] D.R.Clarke // *J. Am. Ceram. Soc.* **70** (1987) 15.

[9] A.L.Kolesnikova, I.A.Ovid'ko and A.B.Reizis // *J. Mater. Proc. Manuf. Sci.* **7** (1999) 5.
[10] I.A.Ovid'ko and A.B.Reizis // *J. Phys. D: Appl. Phys.* **32** (1999) 2833.
[11] J.Horvath // *Defects and Diffusion Forum* **66-69** (1989) 207.
[12] H.-J.Hofler, H.Hahn and R.S.Averback // *Defects and Diffusion Forum* **75** (1991) 195.
[13] L.A. Girifalco and D.O. Welch, *Point Defects and Diffusion in Strained Metals (*Gordon and Breach, 1967).
[14] A.P.Sutton and V.Vitek // *Phil. Trans. Roy. Soc. London* **A 301** (1983) 1.
[15] A.P.Sutton and R.W.Ballufi, *Interfaces in Crystalline Materials* (Clarendon Press, Oxford, 1995).
[16] G.-J.Wang and V.Vitek // *Acta Metall.* **34** (1986) 951.
[17] K.N.Mikaelyan, I.A.Ovid'ko and A.E.Romanov // *Mater. Sci. Eng.* **A 259** (1999) 132.
[18] F.R.N. Nabarro, *Theory of Crystal Dislocations* (Clarendon Press, Oxford, 1967).